Influence of the Crystalline State on Photoinduced Dynamics of Photoactive Yellow Protein Studied by Ultraviolet-Visible Transient Absorption Spectroscopy

Sergey Yeremenko,* Ivo H. M. van Stokkum,† Keith Moffat,‡ and Klaas J. Hellingwerf*

*Swammerdam Institute for Life Sciences, University of Amsterdam, 1018 WY Amsterdam, The Netherlands; †Department of Biophysics, Faculty of Sciences, Vrije Universiteit, 1081 HV Amsterdam, The Netherlands; and ‡Department of Biochemistry and Molecular Biology, and the Institute for Biophysical Dynamics, University of Chicago, Chicago, Illinois 60637

ABSTRACT Time-resolved ultraviolet-visible spectroscopy was used to characterize the photocycle transitions in single crystals of wild-type and the E-46Q mutant of photoactive yellow protein (PYP) with microsecond time resolution. The results were compared with the results of similar measurements on aqueous solutions of these two variants of PYP, with and without the components present in the mother liquor of crystals. The experimental data were analyzed with global and target analysis. Distinct differences in the reaction path of a PYP molecule are observed between these conditions when it progresses through its photocycle. In the crystalline state i), much faster relaxation of the late blue-shifted photocycle intermediate back to the ground state is observed; ii), this intermediate in crystalline PYP absorbs at 380 nm, rather than at 350–360 nm in solution; and iii), for various intermediates of this photocycle the forward reaction through the photocycle directly competes with a branching reaction that leads directly to the ground state. Significantly, with these altered characteristics, the spectroscopic data on PYP are fully consistent with the structural data obtained for this photoreceptor protein with time-resolved x-ray diffraction analysis, particularly for wild-type PYP.

INTRODUCTION

A key aspect in the understanding of the function of enzymes in particular, and proteins in general, is detailed insight into the structural transitions that underlie their function. When studied at the ensemble level, such information is only obtainable from presteady-state kinetics analyses. As enzyme-mediated catalysis typically has a turnover time on the order of milliseconds, the structural techniques that can contribute to this important area of research in the life sciences will have to have at least microsecond time resolution. Trapping states chemically and/or physically is an alternative, but this approach is complicated by difficulties in limiting the number of trapped states to only one or a few (1,2). Studies at the single molecule level would be another alternative, but none of the currently available high-resolution structural techniques (e.g., x-ray diffraction) can be applied in that approach.

X-ray diffraction analysis is the technique that provides by far the most detailed (atomic) resolution in structural studies in the life sciences. This technique has undergone astounding improvements in time resolution during the past decades. Through the use of the intense pulsed x-ray beams which have become available through the use of synchrotron facilities, the time resolution in x-ray diffraction has improved to better than one nanosecond (3); even higher temporal resolution is under development (4). These studies also require of course (ultra)fast activation of the system under study, which is most easily achieved with naturally photoactivated systems. Several such systems are known (e.g., myoglobin, bacteriorhodopsin), but by far the most detailed information has become available for the blue-light photosensory protein from *Halorhodospira halophila*, photoactive yellow protein or PYP (3,5–8).

These studies initially revealed structures related to those of a late (5) and an early (9,10) intermediate. However, further improvements of the data analysis in the Laue-diffraction approach (i.e., diffraction analysis with polychromatic x-rays) have allowed the application of 'global' analyses procedures to such data sets (11–13). As a result, the possibility of proposing a detailed chemical kinetic mechanism describing the partial reactions that jointly make up the photocycle of PYP has emerged, both for wild-type PYP (14,15) and its E-46Q mutant (16).

Nevertheless, when one zooms in on specific structural features of an enzyme, e.g., in its active site, spectroscopic techniques often can provide much higher spatial resolution. Various vibrational spectroscopies provide subangstrom resolution of particular interatomic distances and dihedral angles (17). This is particularly relevant to enzyme activity, because an orders of magnitude effect on the acceleration of the rate of the reaction catalyzed by that particular enzyme (18) can be produced by subangstrom alteration of key interatomic distances.

Ideally, therefore, one would want to combine information on a specific enzyme-reaction mechanism obtained by both structural and spectroscopic techniques. This is straightforward if the reaction under study proceeds identically when

Submitted September 19, 2005, and accepted for publication January 26, 2006.

Address reprint requests to Klaas J. Hellingwerf, Laboratory for Microbiology, Swammerdam Institute for Life Sciences, Nieuwe Achtergracht 166, NL-1018 WV Amsterdam, The Netherlands. Tel.: 31-20-525-7055; Fax: 31-20-525-7056; E-mail: K.Hellingwerf@science.uva.nl.

0006-3495/06/06/4224/12 $2.00

doi: 10.1529/biophysj.105.074765

the protein is present in aqueous solution and in a crystalline lattice. Evidence has been provided that this condition may not be fulfilled in the light-induced reaction undergone by PYP (19,20). For this reason we have set up a system that allows ultraviolet-visible (UV-vis) characterization of the photocycle transitions of PYP with microsecond time resolution on single crystals of PYP in space group $P6_5$. We studied wild-type protein and a mutant form in which the glutamic acid residue at position 46 is replaced by a glutamine (i.e., E-46Q). In wild-type PYP the carboxyl group of E-46 donates a proton to the chromophore in the step that leads to pB′ formation. Therefore the E-46Q mutant is of interest for studies of the mechanism of chromophore protonation. The E-46Q mutant has also been extensively studied with time-resolved crystallography.

Our analysis shows distinct differences in the reaction path of a PYP molecule when it progresses through its photocycle under the two conditions specified above. In the crystalline state, i), significantly faster relaxation to the ground state is observed; ii), the late blue-shifted intermediate in crystalline PYP absorbs maximally at 380 nm, rather than at 350–360 nm as is does in solution; and iii), for various photocycle intermediates, the forward reaction competes with a relaxation reaction that leads directly to the ground state of PYP.

MATERIALS AND METHODS

Protein expression, purification, and sample preparation

Wild-type PYP and E-46Q mutant protein were overproduced, reconstituted with chromophore, and purified as described elsewhere (21). Crystals in space group $P6_5$ were obtained by the vapor diffusion method after 1–2 days of incubation at 20°C, with equal volumes of ~20–30 mg/mL solution of PYP and 40% (wt/vol) polyethylene glycol (PEG) 2000 precipitant in 100 mM 2-(*N*-morpholino)-ethanesulphonic acid (MES), pH 6.5. The same protein in pure MES buffer (pH 6.5) at a concentration of ~25 μM was used for measurements in dilute solution.

Time-resolved spectroscopy

Microsecond-to-millisecond transient absorption spectroscopy was carried out using a flash-photolysis spectrometer (LP900, Edinburgh Instruments, Livingston, UK) equipped with a Q-switched Nd:YAG laser (Continuum Surelight, Continuum, Santa Clara, CA), an optical parametric oscillator to provide the frequency tuning, and a Xe-flash lamp for probing. The excitation pulse duration was ~6 ns. Time-gated difference spectra were collected using a charge-coupled device (CCD) detector array equipped with an image intensifier. Single wavelength spectral kinetics were measured through the use of a photomultiplier connected to an oscilloscope (TDS 340A, Tektronix, Ismaning, Germany). The optical path length of dilute samples was 1 cm. A commercial microspectrophotometer unit (4DX Systems, Uppsala, Sweden) (22) for spectroscopic measurements on single protein crystals was coupled with the probing light of the flash-photolysis spectrometer by means of an optical fiber while the pump beam from the laser was directly focused onto the sample. The pump energy was empirically set at a level, not exceeding a few microjoules, such that no significant irreversible photobleaching of the sample was observed during the experiment (see below for details).

Transient absorption measurements on the solution samples were performed using the kinetic mode of the spectrometer, in which the absorption changes in a narrow wavelength interval are monitored with a photomultiplier. With the type of the setup used, this regime allows for a faster measurement and better temporal sampling. The scans were performed with a wavelength step of 10 nm and spectral resolution of ~3 nm in the spectral range from 340 to 500 nm. Since the probing light intensity cannot be significantly reduced in time-resolved measurements with the photomultiplier, the recovery rate observed in our measurements is slightly increased as a result of the branching reaction induced by the probing light (23). To correct for this effect we also performed a scan of longer timescales, associated with recovery of the ground state, using a CCD camera equipped with an image intensifier, which allowed us to significantly reduce the probing light intensity. In this way the experimental data are corrected for the influence of the probing light on the photoreaction.

Since the intensity of the probing light is greatly reduced in the microspectrophotometer configuration, the CCD camera, equipped with an image intensifier, is employed for the crystalline samples. Thus, the transient absorption of single crystals was measured in the form of time-gated spectra; ~40 time-gated spectra were measured in the time interval from 1 μs to 250 ms. Temporal resolution was of the order of 1–5 μs for both types of measurements.

All manipulations with the crystals were performed in a stream of nitrogen gas saturated with water vapor. The crystals were mounted in 1-mm glass capillaries (Hampton Research, Laguna Niguel, CA) partially filled with the crystallization mother liquor to provide constant humidity conditions and to prevent dehydration of the crystals in the course of the experiments. Additionally, crystals were protected from dehydration by soaking in paraffin oil (Hampton Research). The measurements were performed at 20°C.

Data analysis

The time-resolved data were analyzed using methodology of global and target analysis as described in van Stokkum et al. (24). Target analysis implies that the two-dimensional data set, of time wavelength versus absorption difference, is analyzed simultaneously using a predefined kinetic scheme with n intermediates and unknown kinetic parameters, which describes the evolution of the system after photoexcitation. Thereafter we denote the kinetic scheme of the photoreaction with a specified number of intermediates and particular kinetic relations between them as the photoreaction mechanism. The time-resolved difference absorption spectrum of the sample $\psi(t,\lambda)$ is represented as a superposition of the contributions of the n different components:

$$\psi(t,\lambda) = \sum_{i=1}^{n} c_i(t)\varepsilon_i(\lambda), \tag{1}$$

where $c_i(t)$ and $\varepsilon_i(\lambda)$ denote, respectively, the concentration and the difference spectrum of ith component. The corresponding rate equations, describing the kinetic scheme and the relations between the different components, have the following general form:

$$\frac{d}{dt}c(t) = Kc(t) + j(t), \tag{2}$$

where $c(t)$ is the vector that contains the concentration of the components; K is the matrix containing the rates; and the vector $j(t)$ contains additional input into the system. In our fit we used the shape of the ground state spectrum as an input parameter, since it can be readily measured separately using the same experimental setup. We retained only its amplitude as a fitting parameter. We also constrained the spectrum of the blue-shifted intermediate state to be zero at wavelengths above 430 nm, as justified by previous experiments and data analysis (25).

In each fitting session, the kinetic reaction mechanism is tested on several models starting from a simple linear sequence of states and increasing their complexity by introduction of branching reactions or equilibria when the data demonstrate necessity for additional complexity. Apart from the magnitude

of residuals χ^2), an important additional parameter of the fitting quality is the adequacy with which the respective spectral bands are described. That is, only those fitting results which led to physically meaningful amplitudes and shapes of spectral bands of intermediate states were considered.

RESULTS

Ground state absorption

The ground state absorption spectra of wild-type PYP and its site-directed mutant derivative E-46Q are shown in Fig. 1. The red line represents the spectrum of the protein in solution, whereas the spectra of the protein in the crystalline state are shown in black. The blue lines depict the laser excitation spectrum for measurements on (single) crystals. Adjusting this excitation spectrum to the wing of the chromophore absorption band of PYP allows more uniform excitation of the sample that has a very high optical density at the maximum of this absorption band (see also Ng et al. (26)). The absorption spectra of single crystals of PYP were measured with plane-polarized probing light. This allows the optical density of the crystal to be reduced in the UV-vis spectral region for the measuring beam by orienting the polarization plane perpendicular to the long axis of the crystal, which contains the sixfold crystallographic axis of symmetry. The polarization plane is thus perpendicular to the averaged orientation of the chromophore transition dipole moment. All measurements, presented in this work, have been performed with the plane of polarization of the probing light oriented perpendicularly to the long axis of the crystal. Further lowering of the crystal optical density can be achieved by controlling the crystal morphology as shown in Kort et al. (27). In our measurements on (single) crystals the absorption at the peak maximum of the *p*-coumaric acid chromophore in the spectrum of the ground state of PYP did not exceed 1.2. The spectra of the crystalline samples are slightly red-shifted (by ~3–4 nm) with respect to the spectra of PYP in solution, whereas their width and the overall shape are very similar (Fig. 1). This is fully in agreement with earlier observations (26,27). Slightly higher absorption in the blue wing of the polarized UV-vis spectrum in the crystalline samples (particularly in E-46Q) is most probably due to the different mutual orientation of the chromophore transition dipole moment and the transition dipole moment of aromatic residues of the protein responsible for the absorption band centered at ~280 nm and/or small contributions due to light scattering.

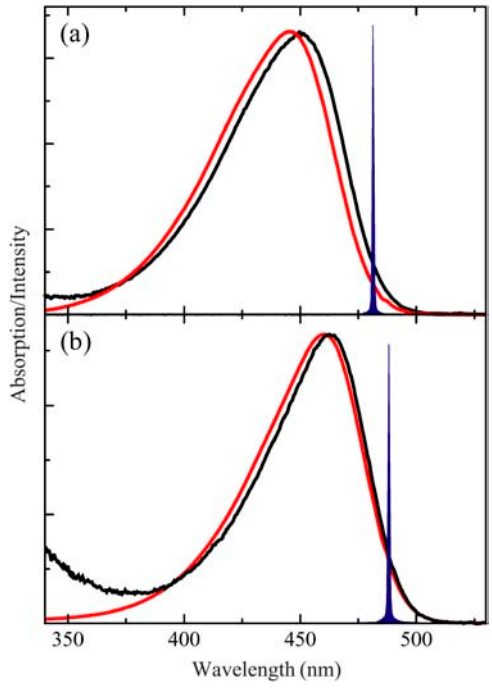

FIGURE 1 Ground state absorption spectrum of wild-type PYP (*a*) and the E-46Q mutant (*b*) in (dilute) solution (*red lines*) and in a crystalline lattice (*black lines*). The blue peak depicts the laser excitation spectrum for the crystalline samples. The spectra of the crystalline samples were measured with a polarized probe beam having the polarization plane oriented perpendicularly to the long axis of the crystal.

Transient absorption

To allow direct comparison of the light-induced absorption changes in PYP in solution and in the crystalline state and of wild-type PYP and its E-46Q mutant, it is convenient to examine transient absorption changes at several key wavelengths. Temporal evolution of the absorption at 490 nm (500 nm for E-46Q), 380 nm (350 nm for PYP samples in solution), and 450 nm (460 nm for E-46Q) is shown in Fig. 2, *a–c*. Note that the transients are normalized to provide better comparison between different samples. Transients at these wavelengths largely reflect the decay of the absorption arising from the red-shifted state pR (Fig. 2 *a*), formation and decay of the absorption arising from the blue-shifted state pB (Fig. 2 *b*), and the depletion of the ground state absorption and its recovery, respectively (Fig. 2 *c*).

Formation of the red shifted state (pR) is not detectable with the time resolution of the apparatus used for our measurements, since this process takes place on the nanosecond timescale (28–31). Therefore, in Fig. 2 *a*, we can observe only the decay of the pR state in the submillisecond time domain. Correspondingly, the increase in absorption on the blue side of the spectrum reflects the concomitant formation of the blue-shifted state (pB). The rate of decay of pR (and, thus, the rate of formation of pB) is evidently very similar for the crystalline and solution samples but noticeably faster in the E-46Q mutant than in wild-type PYP. These data are in accordance with the results of previous studies (19,25,32–35). However, there is a clear difference between the crystalline protein and the solution sample in the submillisecond time domain. Significant absorption is already present in the crystalline sample at the blue side of the spectrum—the spectral region where pB absorbs—at timescales of the order of several microseconds. This effect is particularly evident for wild-type PYP in the crystal, due to the relatively slow rate of the

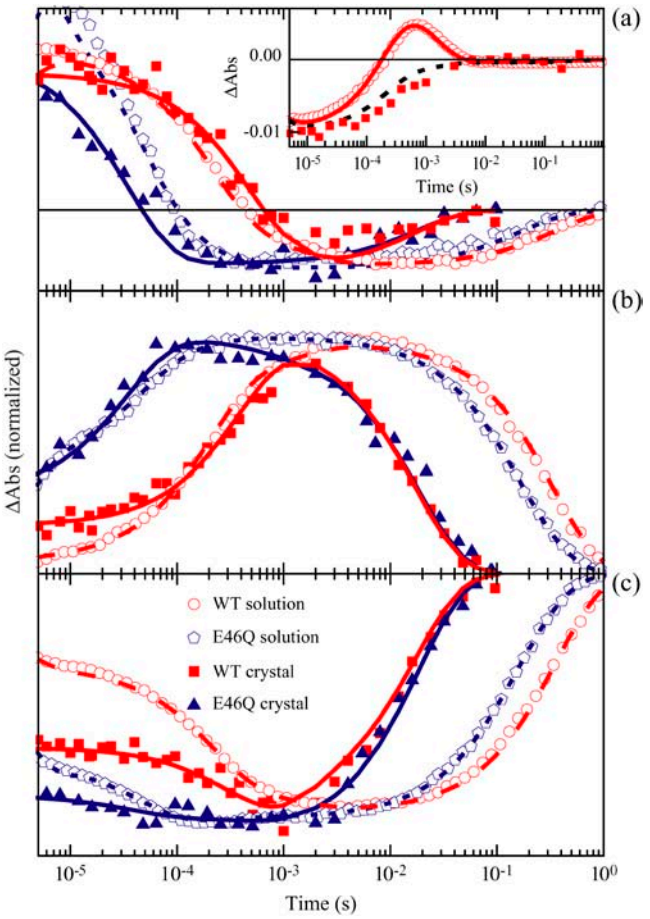

FIGURE 2 Kinetics of the absorption changes of wild-type and E-46Q PYP in the wavelength range 490–500 nm (*a*), 350–380 nm (*b*), and 450–460 nm (*c*). The open symbols represent the data obtained with a dilute solution, whereas the solid symbols are data obtained with single crystals. The results corresponding to wild-type protein are given in red, whereas the results for the E-46Q mutant protein are given in blue. Lines of these respective colors represent the optimal fit to the results obtained (see text for details). In the inset in panel *a*, transient absorption traces of wild-type protein in solution (*open circles*) and in the crystalline state (*solid squares*) at a wavelength of 382 and 410 nm, respectively, are shown. The solid and dashed line represent the best fit of solution data with the full model (see text and Fig. 3 *a* for details) and a model calculation with identical spectra of the pB- and pB′ intermediates, respectively.

ground state recovery under these conditions. The presence of absorption at the blue side of the spectrum at such an early timescale can be considered a strong indication of a branching reaction in the pR state, the precursor of pB. Consequently, formation of the pB state occurs on two substantially different timescales.

More differences between wild-type protein in the crystalline state and in solution are apparent in the millisecond timescale, which reflects the phase of the recovery of the ground state of the protein. The crystalline protein recovers the ground state substantially faster than the protein in solution (26,27). Furthermore, there is little difference between the rate of recovery of the E-46Q mutant and wild-type in the crystalline state, whereas in solution the E-46Q protein recovers noticeably faster than wild-type.

Examination of the absorption transients at several key wavelengths allows us to conclude that the photocycle of PYP differs depending on whether the protein is in the crystalline state or dilute solution. To fully characterize the photocycle, i.e., to determine the number, spectra and connectivity of the intermediate states, and the rate coefficients by which these states interconvert, we applied the method of target spectroscopic analysis to the experimental data (24).

Results of the target analysis are presented in Fig. 3 for wild-type PYP and in Fig. 4 for the E-46Q mutant, which compare their photocycles in solution and in the crystalline state. For wild-type PYP in solution, our experimental data can be well described by a model introduced previously (25) (see Fig. 3 *a*). This model includes three key intermediate states in the timescale reported here: an early red-shifted intermediate, pR, and two blue-shifted, pB, intermediates (the first of which is denoted here as pB′). This is the optimal number of intermediate states required to describe our experimental data: No simpler scheme is able to reproduce the data adequately, and addition of more intermediates does not lead to a significant improvement in fit quality. Several earlier experiments indicate more complex dynamics on the nanosecond and early microsecond timescales (2,15,16) and in particular, it has been suggested that there are at least two

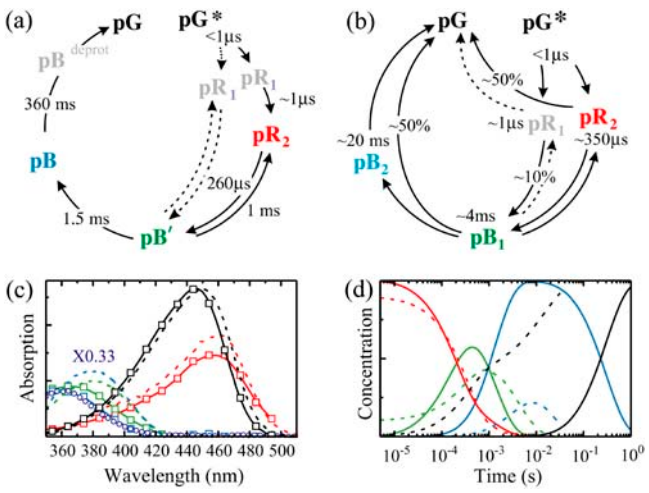

FIGURE 3 Results of the target analysis of wild-type PYP in solution and in the crystalline state. (*a*) Kinetic scheme of the photocycle of wild-type PYP in (dilute) solution. (*b*) Kinetic scheme of the photocycle of wild-type PYP, when present in a crystalline lattice. The states in light color in *a* and *b* have not been characterized in this study. (*c*) Absorption spectra of the intermediate states. Absorption spectra of the long-living intermediate states of the crystalline sample (*green* and *blue dashed lines*) are normalized by a factor of three for the sake of convenience of the comparison with the solution data. (*d*) The temporal evolution of the concentration of each intermediate state. The solid and dashed lines in *c* and *d* represent data obtained with a solution of PYP and with crystalline PYP, respectively. The open squares in *c* represent the actual experimental data points of the solution data, whereas the solid lines are guides to the eye. The open circles depict the absorption of the irreversibly photobleached state.

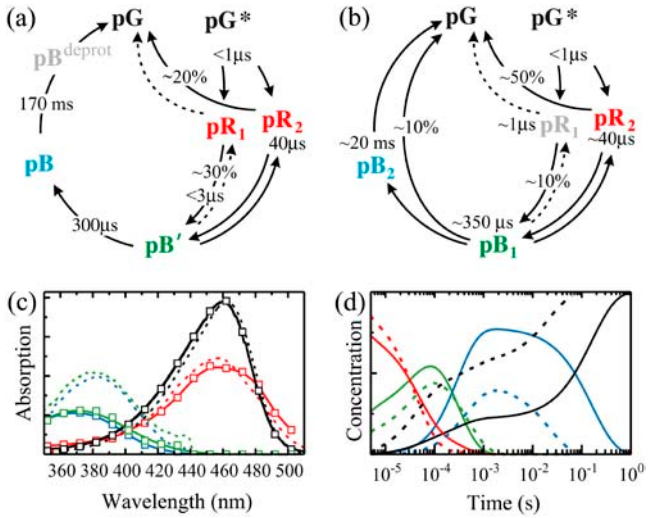

FIGURE 4 Results of the target analysis of the E-46Q mutant of PYP in solution and in the crystalline state. (*a*) Kinetic scheme of the photocycle of the protein in (dilute) solution. (*b*) Kinetic scheme of the photocycle of the protein when present in a crystalline lattice. (*c*) Absorption spectra of the intermediate states. (*d*) The temporal evolution of the concentration of each intermediate state. The dashed lines in *a* and *b* refer to processes for which no reliable quantitative estimates of rates and amplitudes could be obtained. The solid and dashed lines in *c* and *d* represent the solution and the crystalline lattice data, respectively. The open squares in *c* represent the actual experimental data points of the solution data, whereas the solid lines guide the eye. The states in light color have not been characterized in this study. Color code in *c* and *d*: black, pG; red, pR; blue, pB′; and purple, pB.

substates, pR_1 and pR_2, evolving in this time domain. Therefore in the scheme shown in Fig. 3 *a*, we include two red-shifted early intermediates. However, the presence of the shorter-lived of the two cannot be directly verified from our data, since this intermediate is supposed to have a lifetime comparable with the temporal resolution of our setup. Furthermore, the precise kinetic scheme by which these pR intermediates evolve is still far from clear: They may occur sequentially (36,37) and/or in parallel (2,15,16). We depict both possibilities in the scheme in Fig. 3 *a*: sequential evolution of pR_1 and pR_2 and parallel coexistence of the two states with different lifetimes. Our experimental data favor the sequential model, since no submicrosecond formation of the pB state is observed. However, a parallel scheme cannot be fully excluded. Further experiments are required to elucidate the precise kinetic mechanism and the rate coefficients by which intermediates form and decay in this time domain.

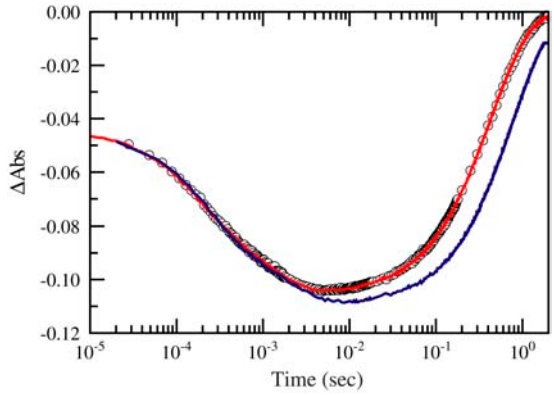

FIGURE 5 Influence of macromolecular crowding on the photocycle of PYP. Symbols represent transient absorption kinetics at 450 nm of a dilute solution of PYP in MES buffer at pH = 7. The red line shows transient absorption kinetics of PYP at 450 nm in solution with ~10 mM BSA, whereas the blue line corresponds to the transient absorption kinetics of a solution of PYP containing PEG 2000 at 200 g/l.

Introducing reversibility between the states pR and pB′ significantly improved the fit quality, in agreement with previous studies (25). No other model, including those with branching in some intermediate states as suggested for crystallographic data (15), could provide a fit of comparable quality. It is relevant to note that at the pH of 6.5 used in this experiment the equilibrium is shifted toward pB′, a state in which the chromophore is protonated. The rate coefficients and the spectra of the intermediate states (Fig. 3 *c*, *solid lines*) obtained in the fit are also in good agreement with the literature (25,32). Our data analysis confirms the presence of the two blue-shifted intermediate states with a mutual spectral shift of ~7 nm (19,25). A transient at 384 nm, a wavelength which corresponds to the isosbestic point between the pB and pG states, very clearly illustrates the transition pB′ → pB (*inset* in Fig. 2 *a*). The transient bleaching present at the early microsecond timescale is due to the induced transmission of the ground state as a result of the transition pG → pR. The recovery of the bleach is related to the formation of the pB′ state, whereas the transient absorption at the early millisecond timescale is related to the transition pB′ → pB. At the millisecond timescale the signal levels off since at this wavelength the absorption increase of pB is compensated by decreased absorption of the pG state. If the signal is simulated according to the full photocycle model shown in Fig. 3 *a* in which no spectral shift during the transition pB′ → pB is assumed to take place (i.e., the spectra of the pB′ and pB intermediates are identical), then no transient absorption is present at the early millisecond timescale. This is illustrated by the dashed line in the inset in Fig. 2 *a*.

The model used to describe the wild-type protein in solution, however, appeared to be unable to adequately describe the data on the same protein in crystalline form. As has been pointed out in the previous section, the early time points of the crystalline samples provide an indication for the existence of a branching reaction in the early pR state at the submicrosecond timescale, which results in the formation of the blue-shifted pB′ state on two substantially different timescales. Moreover, our further analysis shows that not all protein molecules in a crystal that reach the intermediate state with the red-shifted absorption spectrum proceed to the states that have a blue-shifted spectrum; ~50% of the protein molecules decay from the pR state directly to the ground state (Fig. 3 *b*) and do not pass through any pB state.

In the model describing wild-type PYP in the crystalline state shown in Fig. 3 *b*, we include two coexisting pR states (pR_1 and pR_2), one of which, pR_1, decays on the timescale comparable with our temporal resolution and cannot be reliably detected in our measurement. Consequently, in our simulations, the early pB_1 state was populated directly after the excitation. Our analysis revealed that ~10% of the protein molecules proceed through the pR_1 state. This follows from the amplitude of the absorption of the pB_1 state observed in the crystalline sample at the early microsecond timescale. The lifetime of the longer-lived intermediate state pR_2 is ~350 μs in crystalline PYP, which is comparable to that in solution. The spectrum of the pR_2 state of the crystalline sample is shown in Fig. 3 *c* as a dashed red line. It strongly resembles the spectrum of this state in solution.

Global analysis of the transient absorption data obtained with wild-type PYP in the crystalline state revealed two components with a blue-shifted absorption spectrum, with lifetimes of ~4 ms (pB_1) and ~20 ms (pB_2). The pB_1 and pB_2 states presumably are equivalent to the pB′ and pB states in (dilute) solution. However, to fit the data with adequate quality, the introduction of branching from the pB_1 state at the previous step of the photocycle was required; ~50% of the protein molecules proceed directly to the ground state from the short-lived (initial) blue-shifted intermediate pB_1. In the model of the photocycle for crystalline PYP, we also include a reversible equilibrium between the pR_2 and pB_1 states. Although this does not lead to a dramatic improvement in fit quality, the chemical rationale for reversibility (see Hendriks et al. (25) and Borucki et al. (35) for details), as well as the strong indication for its presence in solution, are incentives to introduce this equilibrium in the model for crystalline PYP. Because the short-lived pR_1 state is not resolved in our experiments, we did not include the equilibrium between the pR_1 and pB_1 states in our simulations. However, the same reasoning as presented above for the transition from the pR_2 to pB_1 states also holds for the transition from pR_1 to pB_1; therefore we cannot exclude the existence of this latter equilibrium.

The spectra of the pB_1 and pB_2 states are very similar in the shape and position of their absorption maxima and differ mainly in the magnitude of their extinction coefficients as shown in Fig. 3 *b*, where they are depicted by green and blue dashed lines. Note the scaling factor of 0.33 for the absorption of pB_1 and pB_2 crystalline intermediates shown in Fig. 3 *c*. The spectra of the blue-shifted intermediate states in solution and in the crystal differ significantly. The absorption maximum of the blue-shifted intermediate in crystalline PYP is at 380 nm, quite different from ~355 to ~360 nm in solution. Furthermore, there is no significant spectral shift between the pB_1 and pB_2 states. The latter point was verified by measurement of a transient at 410 nm, which corresponds to the isosbestic point between the pB_2 and pG states (see *inset* in Fig. 2 *a*). Unlike the sample in solution, the kinetic trace of the crystalline sample shows no transient absorption at the millisecond timescale, which reflects the spectral shift during the pB_1 to pB_2 transition. We have also verified that the positions of the spectral bands of the pB_1 and pB_2 states do not depend on the polarization of the probing light (data not shown). Nevertheless, a form with an absorption spectrum shifted to shorter wavelengths can be generated in the crystal by long exposure to high intensity excitation, which produces irreversible photobleaching. Although the precise nature of this photodecomposition of the protein is not known, the shape and position of the absorption band of the product (*open circles* in Fig. 3 *c*) corresponds to the absorption spectrum of the late pB intermediate of the sample in solution. This suggests that photodecomposition leads to further alteration of the chromophore and protein structures, resulting in chromophore protonation and its exposure to the solvent environment. The difference between the spectra of the photobleached state and the pB intermediate of the crystalline protein emphasizes the relatively smaller blue shift of the absorption spectrum of the latter one.

To compare the dynamics of the protein in the crystalline state and in solution, we display the temporal evolution of the concentration of the intermediate states after photoexcitation in Fig. 3 *d* (crystal, *dashed lines*; solution, *solid lines*). The pR_2 state evolves on similar timescales in both crystal and solution, whereas the presence of a substantial fraction that proceeds through the short-lived pR_1 state in the crystal leads to noticeably faster population of the early pB_1 state in this case. Furthermore, repopulation of the ground state in the crystal has already begun in the microsecond timescale, whereas in solution no such repopulation takes place until the millisecond timescale. Thus, the presence of branching reactions to the ground state from each intermediate state in the crystalline sample leads to decay of the concentration of these states at each step of the photocycle and a corresponding repopulation of the ground state. The lifetime of the early pB_1 state in the crystalline sample is slightly longer than that of the pB′ state in solution. Notwithstanding this, the later pB_2 state in the crystal decays ~10-fold faster than the pB state in solution.

Whereas a generally accepted kinetic model of the photocycle of wild-type PYP in solution is available, a definitive model of the photocycle of the E-46Q mutant is still under discussion (16,35,38). The quality of our experimental data allows revealing additional detail about the photocycle of E-46Q, as shown in Fig. 4 *a*. Global analysis of the transient absorption data demonstrates that at the early microsecond timescale, the E-46Q mutant evolves analogously to wild-type crystalline PYP with two coexisting, red-shifted (pR) intermediates, one of which has a lifetime shorter than the temporal resolution of our setup (<5 μs); ~1/3 of the protein proceeds through the short-lived pR_1 state. As for crystalline wild-type protein, a substantial fraction (~30%) decays from pR directly to the ground state. Whereas the lifetime of the short-lived pR_1 state lies below the time resolution of our setup, the intermediate state pR_2 is well resolved in our

measurements. It decays on the timescale of ~40 μs, which is still almost an order of magnitude faster than the corresponding intermediate in wild-type PYP. We also introduced into this model the equilibrium between the states pR_2 and pB′, which—as in the wild-type protein—noticeably improved the quality of the fit. At the longer timescales the photocycle mechanism is similar to that for the wild-type protein in solution: Two intermediate states, each with a blue-shifted absorption spectrum, decay with time constants of ~300 μs and ~170 ms. The spectra of the intermediate states of E-46Q in solution are shown in Fig. 4 *c* (*solid lines*). The spectrum of the early intermediate pR_2 state in E-46Q is similar to that of the corresponding state in the wild-type protein. It is centered at 460 nm and thus almost fully overlaps with the ground state absorption band, also centered at 460 nm in the E-46Q mutant. The spectra of the two long-lived, blue-shifted photocycle intermediates have very similar shape and amplitude. The absorption spectrum of the pB_1 state is centered at ~373 nm, whereas that of the longer-lived pB_2 state is shifted to a shorter wavelength by ~5 nm. Thus, the latter nearly overlaps with the spectrum of the pB′ intermediate of wild-type PYP.

Analysis of the transient absorption data of the E-46Q mutant in the crystalline state shows that its kinetic photocycle model is similar to that of the crystalline wild-type protein (compare Figs. 3 *b* and 4 *b*). The two pR states may both evolve to the early pB_1 state or decay directly to the ground state without entering the later stages of the photocycle. The lifetime of the pR_2 state is ~40 ms, identical to the corresponding state in solution, whereas the short-lived pR_1 state, through which ~10% of the protein proceeds, decays on a timescale comparable to the temporal resolution of our setup; ~30% of the pB_1 state decays directly to the ground state, whereas the rest evolves into the longest-lived pB_2 state. The lifetime of pB_1 is ~350 ms, which is also very similar to the lifetime of the early blue-shifted pB′ state in solution. The long-lived, blue-shifted intermediate pB_2 in crystals of E-46Q decays to the ground state with a time constant of the order of 20 ms—identical to the crystalline wild-type protein. Recovery of the ground state of crystalline E-46Q protein is several times faster than in solution. However, both are significantly faster than the corresponding processes in wild-type PYP.

The absorption spectra of the intermediate states of the E-46Q mutant, obtained from the global fitting, are shown in Fig. 4 *c* (*dashed lines*). The spectra of pR in the crystalline state and in solution are very similar. The slight differences between them can be ascribed to some uncertainty in the determination of their shapes, due to large overlap with the ground state absorption band. The spectra of the pB_1 and pB_2 states are very similar, as also holds for wild-type PYP in crystalline form. Both are centered at 380 nm, which is ~10–15 nm red-shifted with respect to the spectra of analogous intermediates in the solution samples. Since the kinetic models of the photocycle of the E-46Q mutant in solution and in crystalline form are very similar, the temporal evolution of the concentration of the intermediate states is also comparable. As Fig. 4 *d* shows, the intermediates pR_2 as well as pB_1/pB′ evolve similarly in solution and in the crystal. Minor differences are due to a variation in the fraction of the protein that proceeds to the later stages of the photocycle, rather than recovering directly to the ground state. The major difference between the photocycle of E-46Q in solution and in the crystalline state becomes apparent during the slowest steps of the photocycle, where the rate coefficients for decay of the longest-lived intermediate differ by almost an order of magnitude. In addition, no direct recovery of the ground state from the intermediate pB_1 is observed in the solution sample. Thus, the fraction of the protein molecules that attain the final stage of the photocycle is higher in solution than in the crystalline state.

It is reasonable to argue that the apparent differences in the photocycle of PYP between dilute solution and the crystalline state may be largely due to the other solutes present in the crystallization buffer (i.e., in the mother liquor). The only additional component of this buffer is PEG 2000, which is used as a precipitant in growing crystals (see Materials and Methods). To elucidate the influence of the crystallization buffer on the kinetics of the photocycle transitions, we measured transient absorption kinetics at several representative wavelengths of a solution sample containing wild-type PYP in standard MES buffer supplemented with the cosolute PEG 2000. The concentrations of the last approached the limit of solubility (200 g/l). In such a solution, wild-type PYP demonstrated relatively minor changes in its photocycle with respect to dilute solution (Fig. 5). Specifically, no indications of differences in the absorption spectra or of the kinetics of formation and decay of photocycle intermediates were observed, with the exception that the rate of recovery of the ground state was noticeably slowed in the presence of PEG 2000. Furthermore, its effect in solution is opposite to that in the crystalline state: Recovery of the ground state of PYP in solution is slowed down by the presence of PEG 2000, whereas crystallization considerably increases the rate of recovery.

As has been discussed in the Introduction, macromolecular crowding, i.e., effects related to the steric hindrance by (co)solute macromolecules, may substantially influence protein functioning under conditions in a living cell (39). In most circumstances, proteins constitute the dominant type of macromolecular cosolute. The crystalline state can be considered to represent maximal macromolecular crowding. However, there is a fundamental difference between the crystalline state and a crowded solution, i.e., the static character of the structure of the former and the large number of ordered intermacromolecular interactions. To test the influence of macromolecular crowding on the photocycle of PYP, we performed transient absorption measurements of PYP in solutions containing high concentration of bovine serum albumin (BSA). This protein was chosen because of its trans-

parency in the wavelength region of interest, its availability in large quantities, its high solubility, and the fact that its isoelectric point of 4.8 is close to that of PYP. In solution both proteins thus bear a similar charge, and steric repulsion of equally charged proteins constitutes the main interaction between these macromolecules, as required by the conditions of the experiment. Transient absorption kinetics at 450 nm for PYP in dilute solution and in a solution containing ~10 mM BSA (i.e., close to saturation) are compared in Fig. 5 (*solid line* and *symbols*). There is no significant difference between the absorption kinetics of these two samples. We conclude that in the concentration range used in this experiment, macromolecules which do not interact specifically with PYP do not influence its photocycle, even at high concentration.

DISCUSSION

The application of time-resolved spectroscopy from the microsecond to second timescale has allowed a nearly complete characterization of the PYP photocycle in the crystalline state and its direct comparison with protein dynamics in solution. Furthermore, comparison of wild-type PYP with its E-46Q mutant provided significant details on the nature of signaling state formation in PYP. Global analysis of the experimental data on wild-type PYP revealed substantial differences in the kinetic scheme of the photocycle and its associated rate constants between the crystalline state and solution. The major difference arises from branching to the ground state in each intermediate state of the photocycle in the crystalline protein, which leads to depopulation of the intermediate states. As a result, only about a quarter of the protein that enters the photocycle reaches the state with the longest lifetime, whereas in solution no significant depopulation is observed from these intermediate states. Moreover, the lifetime of the longest-lived intermediate in the photocycle of the crystalline protein is more than an order of magnitude smaller than that of a solution sample.

Despite these readily observable experimental differences, the overall mechanism of the photocycle i.e., the number and nature of the intermediates and the qualitative manner in which they interconvert, remains closely similar in the crystalline proteins and in solution. Even the quantitative differences are not of large energetic significance when viewed in the context of the entire photocycle; a difference in rate coefficients of one order of magnitude corresponds to a difference in free energy of activation of 0.6 Kcal/mole.

Evidence for structural differences between the long-lived state and the ground state of PYP in solution have been detected with a range of experimental techniques, such as Fourier transform infrared spectroscopy, NMR, photoacoustic spectroscopy, and small-angle scattering (19,40–44). Less pronounced, but significant, changes in protein structure were also observed using x-ray crystallographic studies of a photostationary state (5,9,10,15,16,45). Based on the thousands of crystal structures now available, it is generally agreed that static structures in crystals closely resemble those in solution. Nevertheless, no such agreement exists with respect to dynamic, short-lived structures. The data on functional properties in the crystal, such as those in this work which depend on and reflect dynamic structures, are very much more limited.

It is reasonable to assume that the clear experimental differences in the photocycle of PYP in the crystalline state and in solution are consequences of restriction of the structural transformations by static or dynamic steric hindrance from other molecules in the lattice and/or result from the unusual solvent conditions such as relatively low water content in crystalline samples.

Our experiment with macromolecular crowding reveals no influence of the addition of high concentrations of a macromolecular cosolute on the photocycle of PYP. Although the concentration of BSA used in these experiments was ~6 times lower than the concentration of PYP in the crystalline state, it corresponds to a typical intracellular concentration of macromolecules (46). Therefore, we conclude that nonspecific macromolecular crowding in solution hardly influences the photocycle either in vitro or in vivo, whereas crystallization leads to notable changes, especially in kinetics of the photocycle. Nevertheless in vivo, specific influences could be imposed by specific signaling-interaction partners.

The influence of dehydration on the photocycle of PYP has recently been studied in detail by investigating spectroscopic properties of PYP in films with low hydration levels (47). Dehydration substantially affects the function of the protein: Both the mechanism and the kinetics of the photocycle are significantly altered. The systematic study revealed that the effects on the photocycle are largely related to the low water content rather than to high protein concentration. When ~100 water molecules per molecule of PYP are extracted, PYP is functionally fully inactivated. A total of ~200 molecules can be extracted at 0% humidity (47), at which point the number of remaining water molecules is likely to be relatively small. Crystalline PYP contains ~390 water molecules per molecule of PYP in space group $P6_5$ (41.8% solvent content) as used in our experiments here, and ~325 molecules in space group $P6_3$ (37.2% solvent content), as used in the time-resolved crystallographic experiments (5,10,12,14–16). These values are rather close to the low hydration limit estimated by van der Horst et al. (47). Therefore, crystalline PYP might resemble at least partly dehydrated films of PYP. The photocycles of crystalline and dehydrated PYP indeed have some similar features. Specifically, both mesoscopic contexts exhibit a decrease of the quantum yield of pB formation in which some molecules recover directly to the ground state from the pR state, and other molecules recover directly to the ground from the early, blue shifted pB_1 intermediate, thereby bypassing the longer-lived pB_2 state. Both contexts exhibit an increase in the rate of recovery of the ground state and a shift of the ground state absorption

band toward longer wavelength. However, there also are substantial differences between the photocycles of PYP in the crystalline state and in poorly hydrated films, such as noticeable differences in the rate of formation and decay of intermediate states (i.e., the presence of a second, long-lived pR state and a decreased rate of pB formation in poorly hydrated films) and differences in the position of the absorption maxima of intermediate states (i.e., there is no evidence for a red shift of the absorption maximum of the pB state at low hydration relative to a solution sample). Thus, to some extent the differences between the photocycle in crystalline PYP and in solution may arise from the relatively low water content in a crystal. Nevertheless, static and dynamic steric hindrance imposed by close packing of the protein in the crystal lattice must play an additional role. The crystalline environment with its ordered close packing of protein molecules alters the energy landscape, which in turn modifies the pathway of evolution through the photocycle.

The difference in the spectrum of the long-living photocycle intermediates between the crystalline state and in solution samples can be explained by impediments imposed on the structural transformations by the crystalline environment. The blue shift of the spectrum of the pB state, with respect to that of the ground state, is determined by several factors, of which the protonation state of the chromophore is the most important. However, hydrogen-bonding interactions of the chromophore with nearby side chains and its solvation also make a significant contribution. This is illustrated by the further blue shift of the absorption spectrum of the pB state relative to pB′ in solution. Parallel tempering simulations of wild-type PYP in solution (48) demonstrate that in the early pB′ state the already-protonated chromophore remains close enough to neighboring amino acids to participate in hydrogen bonding. In the long-lived pB state the chromophore is fully exposed to solvent and has lost any such hydrogen bonds.

Direct comparison of the structure of a long-lived intermediate determined using x-ray crystallography (5) and parallel tempering simulations under conditions of dilute solution (48) is shown in Fig. 6. In the crystalline sample the chromophore is only partially exposed to solvent and remains close to Arg-52 (see Fig. 6 *a*). In solution the protein undergoes larger conformational changes that lead to full exposure of the chromophore to solvent (see Fig. 6 *b*). This computationally predicted structure has recently been supported experimentally by multinuclear NMR analyses (49). These structural differences may account for the relative red shift of the absorption spectrum of the slowest photocycle intermediate in the crystalline sample with respect to the spectrum of the corresponding state in solution. This red shift is a result of the remaining hydrogen bonding of the chromophore to the Arg-52, as well as its lower solvation by water molecules. The substantially faster recovery of the ground state in the crystalline samples can be similarly explained: The energy barrier for refolding is likely to be lower in the crystalline protein than in solution due to its less extensive structural transformations. As a result, the refolding of the protein in the process of the ground- (or receptor-)state recovery in crystalline sample is faster.

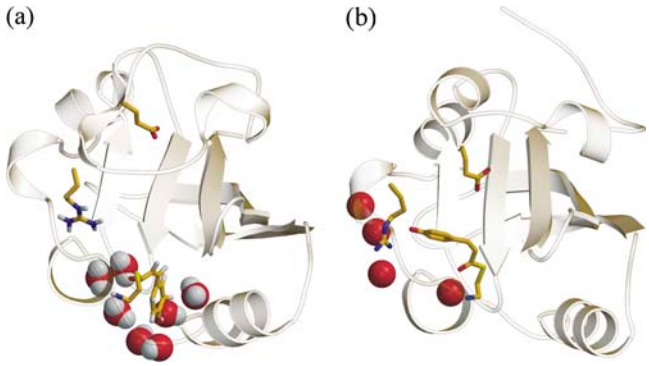

FIGURE 6 Comparison of the structure of the long-living intermediate in the photocycle of PYP obtained under different mesoscopic conditions: (*a*) as determined using x-ray crystallography (formed when PYP is present in a crystalline lattice) (5), and (*b*) as predicted by parallel tempering simulations (48) (formed when PYP is present in dilute solution) and recently confirmed with multinuclear NMR experiments (49). The backbone of the protein is shown in gray, E-46, R-52, and the chromophore as yellow sticks (with *blue* and *red* for N and O atoms), and water molecules interacting with the chromophore as gray/red balls.

The transient absorption measurements on the E-46Q mutant can be explained with the same reasoning used for wild-type PYP. After photoexcitation glutamic acid 46 in wild-type PYP can directly protonate the chromophore phenolate oxygen, whereas glutamine 46 cannot. Furthermore, the hydrogen bond from the chromophore to residue 46 is longer by ~0.3 Å (and presumably weaker) in the E-46Q mutant than in wild-type (50). This shifts the absorption band of the chromophore in the ground state and in the early intermediate states of the photocycle. It may also promote faster structural changes that involve lengthening or rupture of this hydrogen bond to the chromophore.

Our data analysis demonstrates that in both wild-type and E-46Q, two states (i.e., pB′ and pB, of which the latter is ~5 nm blue-shifted with respect to the former) can be identified. Their spectra are slightly shifted to longer wavelength in E-46Q relative to wild-type protein. The spectrum of the pB state in the E-46Q mutant overlaps with that of the pB′ state in wild-type. The existence of two blue-shifted intermediate states in both wild-type and the E-46Q mutant demonstrates the close similarity of the later parts of their photocycles. Formation of the pB′ state reflects protonation of the chromophore (most probably by the solvent in the case of the E-46Q mutant), whereas the transition to the longer-lived pB state reveals certain structural changes of the protein around the chromophore. However, NMR spectroscopy and FTIR measurements suggest that the extent of structural change in E-46Q is smaller than in wild-type (19,51), perhaps due to absence of the negative charge on residue 46 upon formation of the pB states in the E-46Q mutant (51). A smaller extent of

structural change may also contribute to the smaller blue shift of the spectrum of the pB intermediate in the E-46Q mutant relative to wild-type protein.

Finally, it is interesting to compare the results of time-resolved x-ray diffraction measurements (2,15,16,45) with our transient absorption data of the crystalline samples. The great advantage of time-resolved Laue diffraction is that, unlike any spectroscopic technique such as optical or infrared spectroscopies, it allows direct visualization of the dynamics of the entire chemical structure. Moreover, with recent advances in data collection and analysis, the chemical kinetic mechanism and kinetics can be extracted. We previously compared data on crystals of wild-type PYP, which showed remarkable similarity between the right singular vectors obtained from the x-ray diffraction (on crystals in space group $P6_3$) and UV-vis spectroscopic data (on crystals in space group $P6_5$) (52). That is, the time course of the photocycle in the crystal as visualized through these singular vectors is essentially identical whether monitored by x-ray diffraction or UV-vis spectroscopy. More detailed experimental results and extensive analysis of the time-resolved Laue diffraction experiments of wild-type and the E-46Q mutant, published recently, allow comprehensive comparison of these data with the spectroscopic results (15). The kinetic mechanism of the wild-type photocycle and the rate coefficients determined from the crystallographic data (15) almost perfectly match those we obtained independently from the analysis of our spectroscopic experiments. In particular, the number of intermediate states observed by these two experimental methods is identical. Furthermore, branching both at the stage of the early intermediates (in which two coexisting states decay on different timescales) and from the early pB_1 state to the ground state is present in the photocycle mechanisms revealed by both techniques. Thus, the only significant mismatch lies in the presence of branching in the pR state with subsequent direct relaxation to the ground state, for which the UV-vis spectroscopic data provide quite solid evidence. The possibility of this branching reaction was not specifically explored in posterior analysis of the x-ray diffraction data. The remarkable similarity in the right singular vectors noted above means that the x-ray diffraction data are also consistent with the presence of the branching reaction.

In the case of the E-46Q mutant, the results of the UV-vis transient absorption spectroscopy and time-resolved x-ray diffraction (16) differ more substantially. Although the overall photocycle mechanisms demonstrate significant similarity, the assignments of intermediate states and rate coefficients do not match well. In particular the early intermediates, assigned in the crystallographic analysis to pR-like species, decay on a timescale nearly one order of magnitude faster than in our spectroscopic experiments. Temporal evolution of the concentration of the later, pB-like intermediates, determined from the crystallographic data, also does not match well. However, the quality of the experimental crystallographic data for the E-46Q mutant was relatively low: diffraction data at each time point was obtained on a different crystal, and substantial crystal-to-crystal normalization was necessary to piece together the overall time course (12). In comparison, the analogous data for wild-type PYP were obtained with time as the fast variable (15), an approach which greatly reduces systematic errors from time point to time point, and singular value decomposition thus proceeds much more smoothly. We conclude that further work is needed.

In summary, we have compared the photocycles of PYP (wild-type and its E-46Q mutant) in the crystalline state and solution by means of microsecond time-resolved UV-vis spectroscopy. The experimental results reveal clearly detectable, quantitative differences between solution and the crystalline state in the rate of interconversion of intermediate states: Significantly faster relaxation to the ground state is observed in the crystalline samples. The spectral properties of the longest-lived photocycle intermediate state also differ. In the crystalline samples of both wild-type and E-46Q PYP, progress through the photocycle directly competes with a branching reaction leading directly to the ground state, also observed for the E-46Q mutant in solution. The study of the effect of macromolecular crowding, addition of crystallization buffer, and controlled reduction of humidity (47) in combination lead to the conclusion that these differences between the photocycle in a crystalline sample and in solution are likely to arise from a combined effect of dynamic steric hindrance imposed by intermolecular interactions of the protein molecules in the crystal lattice and the relatively low water content in a crystal.

These results stress the importance of the mesoscopic environment for protein function and imply that the presence of a crystal lattice may alter the energy landscape of a protein. Integration of physicochemical data on a particular protein must therefore take proper account of the mesoscopic context in which the data were acquired.

We thank Jos Arents for expert technical assistance, Jocelyne Vreede for providing Fig. 6, and Remco Kort and Michael van der Horst for thoughtful discussions.

This research was supported financially by the Netherlands Foundation of Chemical Research (NWO-CW). K.M. is supported by National Institutes of Health grant GM036452.

REFERENCES

1. Kort, R., K. J. Hellingwerf, and R. B. G. Ravelli. 2004. Initial events in the photocycle of photoactive yellow protein. *J. Biol. Chem.* 279: 26417–26424.
2. Anderson, S., V. Srajer, and K. Moffat. 2004. Structural heterogeneity of cryotrapped intermediates in the bacterial blue light photoreceptor, photoactive yellow protein. *Photochem. Photobiol.* 80:7–14.
3. Moffat, K. 1998. Ultrafast time-resolved crystallography. *Nat. Struct. Biol.* 5(Suppl):641–643.
4. DeCamp, M. F., D. A. Reis, D. M. Fritz, P. H. Bucksbaum, E. M. Dufresne, and R. Clarke. 2005. X-ray synchrotron studies of ultrafast crystalline dynamics. *J. Synchrotron Radiat.* 12:177–192.

5. Genick, U. K., G. E. Borgstahl, K. Ng, Z. Ren, C. Pradervand, P. M. Burke, V. Srajer, T. Y. Teng, W. Schildkamp, D. E. McRee, K. Moffat, and E. D. Getzoff. 1997. Structure of a protein photocycle intermediate by millisecond time- resolved crystallography. *Science*. 275:1471–1475.
6. Moffat, K. 2001. Time-resolved biochemical crystallography: a mechanistic perspective. *Chem. Rev.* 101:1569–1581.
7. Rajagopal, S., and K. Moffat. 2003. Crystal structure of a photoactive yellow protein from a sensor histidine kinase: conformational variability and signal transduction. *Proc. Natl. Acad. Sci. USA.* 100:1649–1654.
8. Ren, Z., D. Bourgeois, J. R. Helliwell, K. Moffat, V. Srajer, and B. L. Stoddard. 1999. Laue crystallography: coming of age. *J. Synchrotron Radiat.* 6:891–917.
9. Genick, U. K., S. M. Soltis, P. Kuhn, I. L. Canestrelli, and E. D. Getzoff. 1998. Structure at 0.85 Å resolution of an early protein photocycle intermediate. *Nature*. 392:206–209.
10. Ren, Z., B. Perman, V. Srajer, T. Y. Teng, C. Pradervand, D. Bourgeois, F. Schotte, T. Ursby, R. Kort, M. Wulff, and K. Moffat. 2001. A molecular movie at 1.8 Å resolution displays the photocycle of photoactive yellow protein, a eubacterial blue-light receptor, from nanoseconds to seconds. *Biochemistry*. 40:13788–13801.
11. Schmidt, M., S. Rajagopal, Z. Ren, and K. Moffat. 2003. Application of singular value decomposition to the analysis of time-resolved macromolecular x-ray data. *Biophys. J.* 84:2112–2129.
12. Rajagopal, S., M. Schmidt, S. Anderson, H. Ihee, and K. Moffat. 2004. Analysis of experimental time-resolved crystallographic data by singular value decomposition. *Acta Crystallogr. D Biol. Crystallogr.* 60: 860–871.
13. Rajagopal, S., K. S. Kostov, and K. Moffat. 2004. Analytical trapping: extraction of time-independent structures from time-dependent crystallographic data. *J. Struct. Biol.* 147:211–222.
14. Schmidt, M., R. Pahl, V. Srajer, S. Anderson, Z. Ren, H. Ihee, S. Rajagopal, and K. Moffat. 2004. Protein kinetics: structures of intermediates and reaction mechanism from time-resolved x-ray data. *Proc. Natl. Acad. Sci. USA.* 101:4799–4804.
15. Ihee, H., S. Rajagopal, V. Srajer, R. Pahl, S. Anderson, M. Schmidt, F. Schotte, P. A. Anfinrud, M. Wulff, and K. Moffat. 2005. Visualizing reaction pathways in photoactive yellow protein from nanoseconds to seconds. *Proc. Natl. Acad. Sci. USA.* 102:7145–7150.
16. Rajagopal, S., S. Anderson, V. Srajer, M. Schmidt, R. Pahl, and K. Moffat. 2005. A structural pathway for signaling in the E46Q mutant of photoactive yellow protein. *Structure*. 13:55–63.
17. Nibbering, E. T. J., H. Fidder, and E. Pines. 2005. Using time-resolved vibrational spectroscopy for interrogation of structural dynamics. *Annu. Rev. Phys. Chem.* 56:337–367.
18. Tonge, P. J., and P. R. Carey. 1992. Forces, bond lengths, and reactivity: fundamental insight into the mechanism of enzyme catalysis. *Biochemistry.* 31:9122–9125.
19. Xie, A., L. Kelemen, J. Hendriks, B. J. White, K. J. Hellingwerf, and W. D. Hoff. 2001. Formation of a new buried charge drives a large-amplitude protein quake in photoreceptor activation. *Biochemistry.* 40:1510–1517.
20. Mano, E., H. Kamikubo, Y. Imamoto, and M. Kataoka. 2003. Comparison of the photochemical reaction of photoactive yellow protein in crystal with reaction in solution. *Spectrosc.-Int. J.* 17:345–353.
21. Kort, R., W. D. Hoff, M. Van West, A. R. Kroon, S. M. Hoffer, K. H. Vlieg, W. Crielaand, J. J. Van Beeumen, and K. J. Hellingwerf. 1996. The xanthopsins: a new family of eubacterial blue-light photoreceptors. *EMBO J.* 15:3209–3218.
22. Hadfield, A., and J. Hajdu. 1993. A fast and portable microspectrophotometer for protein crystallography. *J. Appl. Crystallogr.* 26:839–842.
23. Hendriks, J., I. H. M. van Stokkum, W. Crielaard, and K. J. Hellingwerf. 1999. Kinetics of and intermediates in a photocycle branching reaction of the photoactive yellow protein from Ectothiorhodospira halophila. *FEBS Lett.* 458:252–256.
24. van Stokkum, I. H. M., D. S. Larsen, and R. van Grondelle. 2004. Global and target analysis of time-resolved spectra. *Biochim. Biophys. Acta.* 1657:82–104.
25. Hendriks, J., I. H. M. van Stokkum, and K. J. Hellingwerf. 2003. Deuterium isotope effects in the photocycle transitions of the photoactive yellow protein. *Biophys. J.* 84:1180–1191.
26. Ng, K., E. D. Getzoff, and K. Moffat. 1995. Optical studies of a bacterial photoreceptor protein, photoactive yellow protein, in single crystals. *Biochemistry.* 34:879–890.
27. Kort, R., R. B. Ravelli, F. Schotte, D. Bourgeois, W. Crielaard, K. J. Hellingwerf, and M. Wulff. 2003. Characterization of photocycle intermediates in crystalline photoactive yellow protein. *Photochem. Photobiol.* 78:131–137.
28. Groot, M. L., L. J. van Wilderen, D. S. Larsen, M. A. van der Horst, I. H. M. van Stokkum, K. J. Hellingwerf, and R. van Grondelle. 2003. Initial steps of signal generation in photoactive yellow protein revealed with femtosecond mid-infrared spectroscopy. *Biochemistry.* 42:10054–10059.
29. Baltuška, A., I. H. M. van Stokkum, A. Kroon, R. Monshouwer, K. J. Hellingwerf, and R. van Grondelle. 1997. The primary events in the photoactivation of yellow protein. *Chem. Phys. Lett.* 270:263–266.
30. Vengris, M., M. A. van der Horst, G. Zgrablic, I. H. M. van Stokkum, S. Haacke, M. Chergui, K. J. Hellingwerf, R. van Grondelle, and D. S. Larsen. 2004. Contrasting the excited-state dynamics of the photoactive yellow protein chromophore: protein versus solvent environments. *Biophys. J.* 87:1848–1857.
31. Larsen, D. S., I. H. M. van Stokkum, M. Vengris, M. A. van der Horst, F. L. de Weerd, K. J. Hellingwerf, and R. van Grondelle. 2004. Incoherent manipulation of the photoactive yellow protein photocycle with dispersed pump-dump-probe spectroscopy. *Biophys. J.* 87:1858–1872.
32. Hoff, W. D., I. H. M. van Stokkum, H. J. van Ramesdonk, M. E. van Brederode, A. M. Brouwer, J. C. Fitch, T. E. Meyer, R. van Grondelle, and K. J. Hellingwerf. 1994. Measurement and global analysis of the absorbance changes in the photocycle of the photoactive yellow protein from Ectothiorhodospira halophila. *Biophys. J.* 67:1691–1705.
33. Meyer, T. E., G. Tollin, J. H. Hazzard, and M. A. Cusanovich. 1989. Photoactive yellow protein from the purple phototrophic bacterium, Ectothiorhodospira halophila. Quantum yield of photobleaching and effects of temperature, alcohols, glycerol, and sucrose on kinetics of photobleaching and recovery. *Biophys. J.* 56:559–564.
34. Meyer, T. E., E. Yakali, M. A. Cusanovich, and G. Tollin. 1987. Properties of a water-soluble, yellow protein isolated from a halophilic phototrophic bacterium that has photochemical activity analogous to sensory rhodopsin. *Biochemistry.* 26:418–423.
35. Borucki, B., H. Otto, C. P. Joshi, C. Gasperi, M. A. Cusanovich, S. Devanathan, G. Tollin, and M. P. Heyn. 2003. pH dependence of the photocycle kinetics of the E46Q mutant of photoactive yellow protein: protonation equilibrium between I1 and I2 intermediates, chromophore deprotonation by hydroxyl uptake, and protonation relaxation of the dark state. *Biochemistry.* 42:8780–8790.
36. Chen, E., T. Gensch, A. B. Gross, J. Hendriks, K. J. Hellingwerf, and D. S. Kliger. 2003. Dynamics of protein and chromophore structural changes in the photocycle of photoactive yellow protein monitored by time-resolved optical rotatory dispersion. *Biochemistry.* 42:2062–2071.
37. Losi, A., T. Gensch, M. A. v. d. Horst, K. J. Hellingwerf, and S. E. Braslavsky. 2005. Hydrogen-bond network probed by time-resolved optoacoustic spectroscopy: photoactive yellow protein and the effect of E46Q and E46A mutations. *Phys. Chem. Chem. Phys.* 10:2229–2236.
38. Zhou, Y., L. Ujj, T. E. Meyer, M. A. Cusanovich, and G. H. Atkinson. 2001. Photocycle dynamics and vibrational spectroscopy of the E46Q mutant of photoactive yellow protein. *J. Phys. Chem. A.* 105:5719–5726.
39. Ellis, R. J., and A. P. Minton. 2003. Cell biology: join the crowd. *Nature*. 425:27–28.

40. Imamoto, Y., H. Kamikubo, M. Harigai, N. Shimizu, and M. Kataoka. 2002. Light-induced global conformational change of photoactive yellow protein in solution. *Biochemistry*. 41:13595–13601.

41. Imamoto, Y., Y. Shirahige, F. Tokunaga, T. Kinoshita, K. Yoshihara, and M. Kataoka. 2001. Low-temperature Fourier transform infrared spectroscopy of photoactive yellow protein. *Biochemistry*. 40:8997–9004.

42. Brudler, R., R. Rammelsberg, T. T. Woo, E. D. Getzoff, and K. Gerwert. 2001. Structure of the I1 early intermediate of photoactive yellow protein by FTIR spectroscopy. *Nat. Struct. Biol.* 8:265–270.

43. Rubinstenn, G., G. W. Vuister, F. A. Mulder, P. E. Dux, R. Boelens, K. J. Hellingwerf, and R. Kaptein. 1998. Structural and dynamic changes of photoactive yellow protein during its photocycle in solution. *Nat. Struct. Biol.* 5:568–570.

44. Rubinstenn, G., G. W. Vuister, N. Zwanenburg, K. J. Hellingwerf, R. Boelens, and R. Kaptein. 1999. NMR experiments for the study of photointermediates: application to the photoactive yellow protein. *J. Magn. Reson.* 137:443–447.

45. Anderson, S., V. Srajer, R. Pahl, S. Rajagopal, F. Schotte, P. Anfinrud, M. Wulff, and K. Moffat. 2004. Chromophore conformation and the evolution of tertiary structural changes in photoactive yellow protein. *Structure*. 12:1039–1045.

46. Fulton, A. B. 1982. How crowded is the cytoplasm? *Cell*. 30:345–347.

47. van der Horst, M. A., I. H. M. van Stokkum, N. A. Dencher, and K. J. Hellingwerf. 2005. Controlled reduction of the humidity induces a shortcut recovery reaction in the photocycle of photoactive yellow protein. *Biochemistry*. 44:9160–9167.

48. Vreede, J., W. Crielaard, K. J. Hellingwerf, and P. G. Bolhuis. 2005. Predicting the signaling state of photoactive yellow protein. *Biophys. J.* 88:3525–3535.

49. Bernard, C., K. Houben, N. M. Derix, D. Marks, M. A. v. d. Horst, K. J. Hellingwerf, R. Boelens, R. Kaptein, and N. A. v. Nuland. 2005. The solution structure of a transient photoreceptor intermediate: delta25 photoactive yellow protein. *Structure*. 13:953–962.

50. Anderson, S., S. Crosson, and K. Moffat. 2004. Short hydrogen bonds in photoactive yellow protein. *Acta Crystallogr. D*. 60:1008–1016.

51. Derix, N. M., R. W. Wechselberger, M. A. Van Der Horst, K. J. Hellingwerf, R. Boelens, R. Kaptein, and N. A. Van Nuland. 2003. Lack of negative charge in the E46Q mutant of photoactive yellow protein prevents partial unfolding of the blue-shifted intermediate. *Biochemistry*. 42:14501–14506.

52. Yeremenko, S., and K. J. Hellingwerf. 2005. Resolving protein structure dynamically. *Structure*. 13:4–6.